ChemComm

COMMUNICATION

View Article Online
View Journal

Cite this: DOI: 10.1039/d0cc04484a

Received 29th June 2020,
Accepted 10th August 2020

DOI: 10.1039/d0cc04484a

rsc.li/chemcomm

Oxygen-selective adsorption on high-silica LTA zeolite†

Hanbang Liu,[ab] Danhua Yuan,[a] Guangye Liu,[a] Jiacheng Xing,[ab] Zhongmin Liu [a] and Yunpeng Xu *[a]

The adsorption capacity of O_2 and N_2 on a LTA-type zeolite can be significantly affected by the change of its Si/Al ratio. With the increase in Si/Al ratio and the decrease in the amount of Na^+, the protonated high-silica LTA zeolite changes from being a N_2-selective sorbent to an O_2-selective sorbent to reverse the O_2 and N_2 selectivity.

Both O_2 and N_2 are currently demanded chemicals, and their separation from air is important for numerous industrial and medical applications.[1] The advent of the pressure swing adsorption (PSA) process and porous adsorbents have significantly improved the air separation because of their lower energy consumption. O_2-selective sorbents can be more efficient than N_2-selective materials because the N_2/O_2 ratio in air is approximately 4 (78% *versus* 21%).[2] Many types of O_2-selective porous materials have been successfully developed. Among them, carbon molecular sieves (CMS) separated by kinetic principles have been applied in industry.[3,4] Oxygen-binding transition metal complexes[5,6] and metal–organic frameworks (MOFs)[7–9] can reversibly bind O_2 but are insensitive to N_2. However, the channels of CMS are difficult to accurately control, and the frameworks of transition metal complexes and MOFs are usually unstable. Therefore, the development of new porous O_2 adsorbents that can overcome these problems is of great significance.

Zeolites/molecular sieves, which have the most extensive applications as N_2-selective sorbents, can better interact with N_2 due to the high quadrupole moment of N_2.[10–12] Turning zeolites into O_2-selective adsorbents is difficult, but zeolites have uniform pore apertures, and high hydrothermal and structural stability. At present, ion exchange[13,14] and modification methods of the external surface of zeolites *via* chemical vapor deposition (CVD), chemical liquid deposition (CLD),[15–17] *etc.* have been reported to selectively adsorb O_2 over N_2, which can prevent the kinetic diffusion of N_2 by successfully tailoring their pore apertures. In fact, the number and types of cations in zeolites can be regulated by controlling the Si/Al ratio of zeolites and ion exchange, which will change the electric field gradient of the zeolite framework and affect the quadrupole moment interaction and adsorption amount of N_2,[18] but it may not show an advantage for O_2. To the best of our knowledge, almost no zeolites have been found that successfully achieved a higher O_2 uptake than N_2 using nonkinetic factors.

Here, we pay close attention to the aluminosilicate-type LTA framework zeolite. LTA has a small window size and a large cage, whose pore aperture is close to the kinetic diameters of O_2 (3.5 Å) and N_2 (3.64 Å).[17] The common LTA zeolite is a low-silica material (Si/Al ratio = 1), and its adsorption properties can be changed by ion exchange. For example, the cation exchange of K^+ and Ca^{2+} by NaA (3.8 Å) can obtain 3 A (2.9 Å) and 5 A (4.4 Å),[19] respectively. Prior work has demonstrated that high-silica LTA can be mainly achieved using organic structure-directing agents (OSDAs), such as ZK-4, UZM-9 and ITQ-29.[20–22] The O_2/N_2 selectivity of high-silica LTA zeolites and their ion exchange materials have not been reported in previous studies. In this work, we find that the amounts of N_2 and O_2 adsorbed on LTA zeolites are closely related to their Si/Al ratios, and proton-type high-silica LTA samples have achieved O_2 selectivity. Scheme 1 exhibits the typical framework of LTA and the N_2 and O_2 adsorption on low- and high-silica LTA.

We used density functional theory (DFT) methods to calculate the interaction energies (IEs) between the LTA fragments and N_2 or O_2 molecules (see the ESI†).[23] The commonly used simplified model Si–O–Al(Na) and Si–O–Si fragments were obtained based on the LTA zeolite framework model to fast estimate the possible changes in O_2 and N_2 adsorption of LTA zeolite with Si/Al ratio; all the molecules and fragments were optimized conformational geometries. As demonstrated

[a] National Engineering Laboratory for Methanol to Olefins, Dalian National Laboratory for Clean Energy, Dalian Institute of Chemical Physics, Chinese Academy of Sciences, Dalian 116023, P. R. China. E-mail: xuyunpeng@dicp.ac.cn
[b] University of Chinese Academy of Sciences, Beijing 100049, P. R. China

† Electronic supplementary information (ESI) available: Experimental and characterization details, XRD patterns, TG–DSC curves, N_2 adsorption–desorption isotherms, N_2 and O_2 adsorption isotherms at pressures up to 900 kPa and fitting parameters of the IAST model. See DOI: 10.1039/d0cc04484a

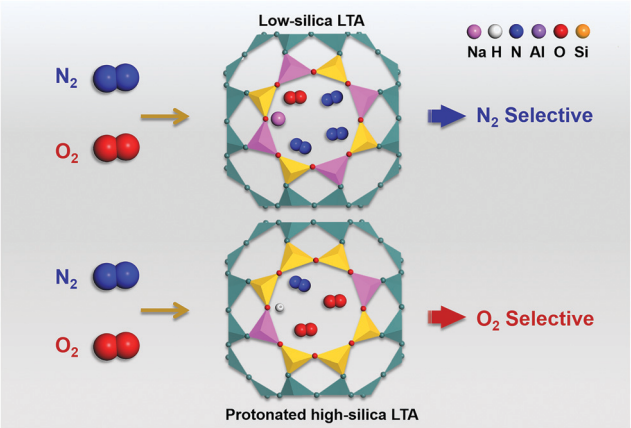

Scheme 1 Schematic illustration of the O_2 and N_2 adsorption processes on low-silica LTA and protonated high-silica LTA.

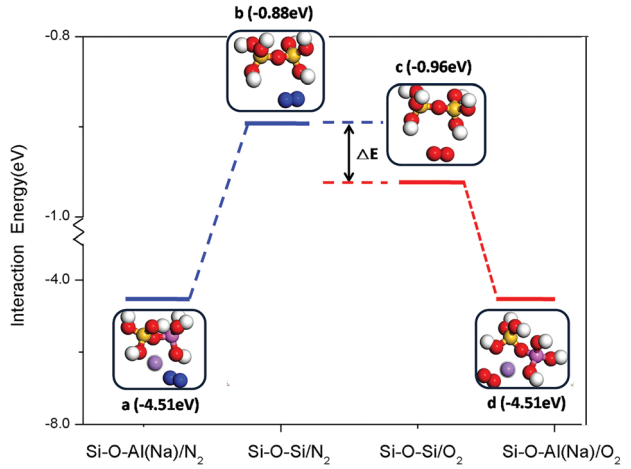

Fig. 1 Optimized conformational geometries and simplified calculated interaction energies of (a) Si–O–Al(Na)/N_2, (b) Si–O–Si/N_2, (c) Si–O–Si/O_2, and (d) Si–O–Al(Na)/O_2 (white: H, red: O, yellow: Si, lavender: Al, purple: Na, and blue: N).

in Fig. 1, the IE between N_2 and Si–O–Si was obviously higher than that between O_2 and Si–O–Si, while the IEs between N_2 or O_2 and Si–O–Al(Na) were almost identical. As a result, DFT calculations suggest that the Si–O–Si fragment in high-silica LTA has stronger electrostatic interactions with O_2 than N_2. In other words, high-silica LTA may result in higher O_2/N_2 selectivity than low-silica NaA.

We obtained NaA (Si/Al ratio = 1.05), ZK-4 (Si/Al ratio = 2.20) and NaUZM-9 (Si/Al ratio = 2.94) and their protonated samples NaA-H, ZK-4-H, and NaUZM-9-H using the reported methods in the existing literature.[21,24,25] The PXRD patterns of the LTA and LTA–H samples show that they had the same typical peaks with LTA topology, which suggests that the LTA samples with high degrees of crystallization were successfully synthesized (Fig. S1, ESI†). Moreover, all the LTA–H samples had high diffraction peak intensities, which indicates that protonated samples have relatively good structural stability (Fig. S2, ESI†). In the DSC

Table 1 Composition and microporous properties of LTA and H-form LTA samples

Sample	Si/Al	Na/Al	S_{BET} m^2 g^{-1}	S_{micro} m^2 g^{-1}	V_m cm^3 g^{-1}
NaA[a]	1.05	0.95	—	—	—
NaA-H	1.06	0.54	459(17)	400	0.23
ZK-4	2.20	0.72	600(22)	568	0.32
ZK-4-H	2.15	0.07	564(21)	485	0.27
NaUZM-9	2.94	0.57	522(19)	465	0.26
NaUZM-9-H	2.81	0.08	514(19)	438	0.25

[a] The pore of NaA is too narrow for N_2 to enter at −196 °C.

curves of these samples (Fig. S4, ESI†), the exothermic peaks above the temperature of 800 °C were attributed to the structural collapse of the LTA zeolites, which shows that NaA began to collapse at 895 °C, but ZK-4 remained stable up to 965 °C, and the collapse temperature of NaUZM-9 was 1010 °C. High-silica LTA had higher collapse temperature than zeolite NaA with low Si/Al ratio. NaA-H, ZK-4-H and NaUZM-9-H had almost identical collapse temperatures to their pristine zeolites. Thus, ZK-4 and NaUZM-9 have higher thermal stability than NaA, and their H-form samples also have good thermal stability.

All the N_2 adsorption–desorption isotherms of the LTA samples at −196 °C are typical type-I sorption isotherms (Fig. S5, ESI†), which correspond to the microporous characteristics of the zeolites. The compositions and microporous properties of these samples are shown in Table 1. Among them, NaA had a scarce N_2 adsorption capacity due to the narrow pore at −196 °C.[26] ZK-4 and NaUZM-9 with high Si/Al ratio had larger window sizes than NaA due to the decrease of Na^+ outside their frameworks. ZK-4 had the largest BET microporous specific surface area (S_{micro} = 568 m^2 g^{-1}) and micropore volume (V_m = 0.32 cm^3 g^{-1}), but NaUZM-9 had slightly smaller S_{micro} (465 m^2 g^{-1}) and V_m (0.26 cm^3 g^{-1}). Meanwhile, when the pristine LTA was modified by ion exchange, with the decrease of Na^+, the pore size of the NaA-H sample increased, which resulted in larger S_{micro} (400 m^2 g^{-1}) and V_m (0.23 cm^3 g^{-1}) than NaA. Both S_{micro} and V_m of the ZK-4-H (S_{micro} = 485 m^2 g^{-1}, and V_m = 0.27 cm^3 g^{-1}) and NaUZM-9 (S_{micro} = 438 m^2 g^{-1}, and V_m = 0.25 cm^3 g^{-1}) samples with extremely low Na^+ contents decreased due to the collapse of their frameworks with the high degree of proton exchange. Obviously, all the protonated samples maintain high S_{micro} and V_m even in acidic conditions.

The adsorption isotherms of pure N_2 and O_2 on LTA samples at 25 °C are compared in Fig. 2. The amounts of N_2 and O_2 adsorbed (100 kPa) on NaA were 0.372 mmol g^{-1} and 0.132 mmol g^{-1}, respectively, which are consistent with the literature description.[17] Regarding the adsorption capacity of N_2, ZK-4 and NaUZM-9 adsorbed less N_2 than NaA, and the N_2 uptake on these samples decreased with the increase in Si/Al ratio. We found that the N_2 capacity of NaUZM-9 was 0.238 mmol g^{-1} at 100 kPa, which was the lowest among the LTA samples. The main reason is that with the increase in Si/Al ratio, the electric field density of the LTA zeolite framework decreases, which reduces the weaker interaction with N_2 that has a high quadrupole moment and ultimately causes the decrease in N_2 uptake on high-silica LTA. However, the O_2 uptake on high-silica LTA zeolite was different from the N_2 uptake: both ZK-4 and NaUZM-9 had higher O_2

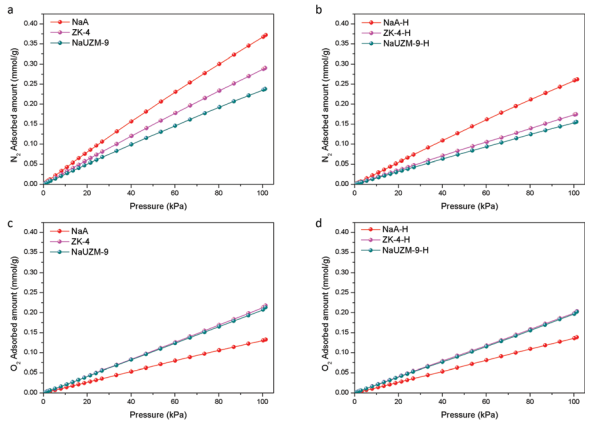

Fig. 2 N_2 adsorption isotherms of the LTA (a) and LTA–H (b) samples at 25 °C; O_2 adsorption isotherms of the LTA (c) and LTA–H (d) samples at 25 °C.

capacity than NaA, which was contrary to the behavior of N_2 adsorbed on these samples. The ZK-4 sample had the highest capacity of O_2 at 100 kPa (0.218 mmol g^{-1}), which was slightly higher than NaUZM-9, whose O_2 uptake at 100 kPa was 0.213 mmol g^{-1}, and both of them were higher than the amount of O_2 adsorbed on NaA, which had never been found in previous studies. We believe that due to the increase in S_{micro} and V_m of high-silica LTA, more O_2 can be adsorbed, and ZK-4 with the largest S_{micro} and V_m has the highest O_2 uptake.

To further reduce the interaction between extra-framework cations of LTA and N_2, we used ion exchange to replace Na^+ with protons, and tested the adsorption capacity of N_2 and O_2 on the protonated LTA–H samples at 25 °C. We found that the N_2 uptakes on all the LTA–H samples conspicuously decreased after Na^+ was replaced by protons. However, the variation of the O_2 uptake was much slighter than that of N_2. For the NaA-H sample, the adsorption capacity of N_2 (0.262 mmol g^{-1}, 100 kPa) remained significantly higher than that of O_2 (0.138 mmol g^{-1}, 100 kPa) even if some of the Na^+ were replaced by protons. For ZK-4-H, the difference in adsorption amounts of N_2 (0.174 mmol g^{-1}, 100 kPa) and O_2 (0.203 mmol g^{-1}, 100 kPa) was not obvious. Nevertheless, the O_2 uptake (0.202 mmol g^{-1}, 100 kPa) on the NaUZM-9-H sample was significantly higher than the N_2 uptake (0.155 mmol g^{-1}, 100 kPa), which is the opposite for the N_2-selective NaA-H. For the first time, proton-type zeolites are observed to have higher O_2 uptake than N_2 without tailoring their pore apertures. In addition, the O_2/N_2 selectivity of LTA zeolites and their proton-type samples at 25 °C were calculated by the ideal adsorbed solution (IAST) theory[27] and are shown in Fig. 3a. As we observed, for the pristine LTA, the O_2/N_2 selectivity gradually increased with the increase in Si/Al ratio but remained below 1, which implies that the N_2 uptake was higher than O_2. However, the O_2/N_2 selectivity of all protonated LTA–H samples was higher than that of the pristine LTA samples and increased with the increase in Si/Al ratio. Additionally, the ZK-4-H and NaUZM-9-H with high Si/Al ratio had O_2/N_2 selectivity above 1; in particular, the selectivity of NaUZM-9-H was 1.32 (100 kPa). The adsorption isotherms of N_2 and O_2 at 25 °C and the pressures up to 900 kPa are shown in Fig. S6 (ESI†), and the O_2 uptakes on high-silica LTA–H were still higher than the N_2 uptakes. At present, the priority of zeolites to adsorb O_2 to N_2 is mainly achieved by controlling the pore size and adsorption rate. The higher O_2 equilibrium adsorption amount than that of N_2 controlled by the nonkinetic factors has important significance.

As described above, we tested the N_2 and O_2 adsorption capacity of Na and proton-type LTA with different Si/Al ratios. The results have strong regularity and are consistent with our DFT calculations. For the pristine LTA, the increase in Si/Al ratio and the addition of OSDAs causes a continuous decrease in the number of Na^+, which results in a lower electric field gradient in them and weakens the interaction with N_2. In contrast, O_2 is not significantly affected by that, and the O_2 uptake increases due to the increase in the specific surface area and the pore volume of high-silica LTA. However, due to the weak interaction with the framework electric field of the zeolites, the adsorption amount of O_2 remains lower than that of N_2. For the proton-type LTA zeolites obtained by ion exchange, their number of extraframework Na^+ is further reduced. At this time, the influencing factor of adsorption capacity mainly depends on the

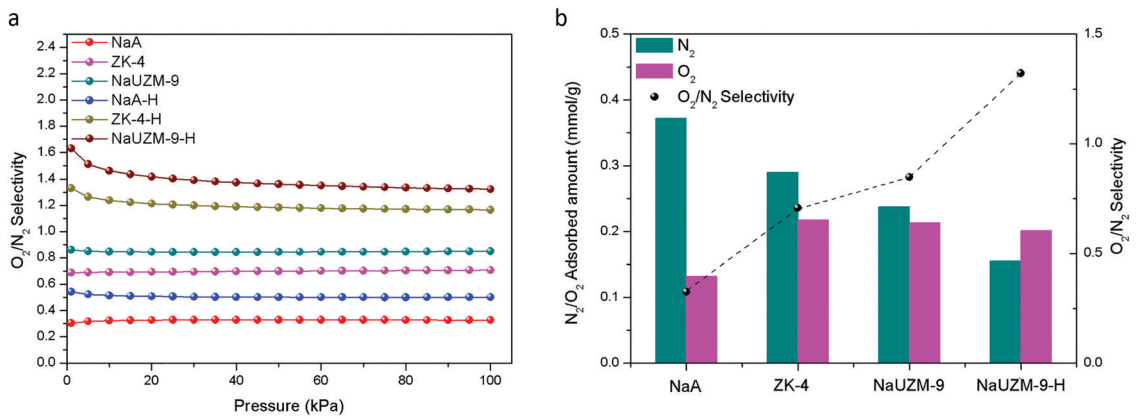

Fig. 3 (a) IAST-predicted selectivity for O_2/N_2 mixtures (21 : 79) on the LTA and LTA–H samples at 25 °C. (b) N_2/O_2 uptake and selectivity of the LTA and NaUZM-9-H samples at 25 °C and 100 kPa.

interaction between N_2 and their framework atoms. From the simulation results in Fig. 1, we find that when the Si–O–Si fragment interacts with N_2 and O_2, the IE of Si–O–Si/O_2 (−0.96 eV) is lower than that of Si–O–Si/N_2 (−0.88 eV), which indicates that the binding ability of O_2 on the Si–O–Si fragment is stronger. O_2 has more advantage when interacting with high-silica LTA samples due to the Si–O–Si fragment in them. Therefore, the high-silica LTA samples with a Si–O–Si fragment have higher O_2 adsorption capacity than N_2 adsorption if the amount of Na^+ is sufficiently small. As shown in Fig. 3b, the O_2/N_2 selectivity of NaUZM-9-H with the highest Si/Al ratio is 1.32 at 100 kPa, which is higher than those of NaUZM-9 and other low-silica LTA samples. At present, the O_2/N_2 selectivity of O_2-selective zeolites obtained by adjusting the pore size of NaA with the more refined CLD method is approximately 1.6 at 100 kPa,[17] which implies that a more excellent separation effect can be obtained based on high-silica LTA–H because of their lower N_2 uptake and higher O_2 uptake. The protonated LTA with high silica content can be used as a new type of selective adsorbent for O_2 adsorption.

In conclusion, we synthesized LTA samples with different Si/Al ratios and tested their N_2 and O_2 adsorption properties. The results show that ZK-4 and NaUZM-9 have higher O_2 adsorption capacity than NaA zeolite, while their N_2 uptakes decrease with the increase in Si/Al ratio, which is not found in other zeolites. The proton-exchanged LTA–H samples with a Si–O–Si fragment and less Na^+ have lower N_2 uptakes, and the O_2/N_2 selectivity of NaUZM-9-H is 1.32 at 100 kPa, which shows a certain potential on O_2-selective air separation.

The work was supported by the National Natural Science Foundation of China (Grant No. 21802136).

Conflicts of interest

There are no conflicts to declare.

Notes and references

1 R. T. Yang, *Adsorbents - fundamentals and applications*, Wiley, New York, 2003.
2 A. Jayaraman, R. T. Yang, S. H. Cho, T. S. G. Bhat and V. N. Choudary, *Adsorption*, 2002, **8**, 271–278.
3 H. Juntgen, K. Knoblauch and K. Harder, *Fuel*, 1981, **60**, 817–822.
4 S. P. Nandi and P. L. Walker, *Sep. Sci. Technol.*, 1976, **11**, 441–453.
5 D. Chen, A. E. Martell and Y. Z. Sun, *Inorg. Chem.*, 1989, **28**, 2647–2652.
6 N. D. Hutson and R. T. Yang, *Ind. Eng. Chem. Res.*, 2000, **39**, 2252–2259.
7 E. D. Bloch, W. L. Queen, M. R. Hudson, J. A. Mason, D. J. Xiao, L. J. Murray, R. Flacau, C. M. Brown and J. R. Long, *Angew. Chem., Int. Ed.*, 2016, **55**, 8605–8609.
8 E. D. Bloch, L. J. Murray, W. L. Queen, S. Chavan, S. N. Maximoff, J. P. Bigi, R. Krishna, V. K. Peterson, F. Grandjean, G. J. Long, B. Smit, S. Bordiga, C. M. Brown and J. R. Long, *J. Am. Chem. Soc.*, 2011, **133**, 14814–14822.
9 D. J. Xiao, M. I. Gonzalez, L. E. Darago, K. D. Vogiatzis, E. Haldoupis, L. Gagliardi and J. R. Long, *J. Am. Chem. Soc.*, 2016, **138**, 7161–7170.
10 S. A. Peter, J. Sebastian and R. V. Jasra, *Ind. Eng. Chem. Res.*, 2005, **44**, 6856–6864.
11 G. Sethia, R. S. Pillai, G. P. Dangi, R. S. Somani, H. C. Bajaj and R. V. Jasra, *Ind. Eng. Chem. Res.*, 2010, **49**, 2353–2362.
12 S. U. Rege and R. T. Yang, *Ind. Eng. Chem. Res.*, 1997, **36**, 5358–5365.
13 M. Iwamoto, K. Yamaguchi, Y. Akutagawa and S. Kagawa, *J. Phys. Chem.*, 1984, **88**, 4195–4197.
14 S. M. Kuznicki, V. A. Bell, S. Nair, H. W. Hillhouse, R. M. Jacubinas, C. M. Braunbarth, B. H. Toby and M. Tsapatsis, *Nature*, 2001, **412**, 720–724.
15 C. D. Chudasama, J. Sebastian and R. V. Jasra, *Ind. Eng. Chem. Res.*, 2005, **44**, 1780–1786.
16 M. Niwa, K. Yamazaki and Y. Murakami, *Ind. Eng. Chem. Res.*, 1991, **30**, 38–42.
17 Y. Wang and R. T. Yang, *ACS Sustainable Chem. Eng.*, 2019, **7**, 3301–3308.
18 Y. Guo, T. Sun, Y. Gu, X. Liu, Q. Ke, X. Wei and S. Wang, *Chem. – Asian J.*, 2018, **13**, 3222–3230.
19 B. W. Boal, J. E. Schmidt, M. A. Deimund, M. W. Deem, L. M. Henling, S. K. Brand, S. I. Zones and M. E. Davis, *Chem. Mater.*, 2015, **27**, 7774–7779.
20 G. T. Kerr, *Inorg. Chem.*, 1966, **5**, 1537–1539.
21 G. J. Lewis, M. A. Miller, J. G. Moscoso, B. A. Wilson, L. M. Knight and S. T. Wilson, *Stud. Surf. Sci. Catal.*, 2004, **154**, 364–372.
22 A. Corma, F. Rey, J. Rius, M. J. Sabater and S. Valencia, *Nature*, 2004, **431**, 287–290.
23 Y. Wu, D. Yuan, D. He, J. Xing, S. Zeng, S. Xu, Y. Xu and Z. Liu, *Angew. Chem., Int. Ed.*, 2019, **58**, 10241–10244.
24 R. W. Thompson and M. J. Huber, *J. Cryst. Growth*, 1982, **56**, 711–722.
25 T. Kodaira and T. Ikeda, *J. Phys. Chem. C*, 2010, **114**, 12885–12895.
26 M. Palomino, A. Corma, F. Rey and S. Valencia, *Langmuir*, 2010, **26**, 1910–1917.
27 A. L. Myers and J. M. Prausnitz, *AlChE J.*, 1965, **11**, 121–127.

